



A comparative study of Mesenchymal Stem Cells transplantation approach to antagonize age-associated ovarian hypofunction with consideration of safety and efficiency



Lingjuan Wang^{a,1}, Qiaojuan Mei^{b,1}, Qin Xie^a, Huiying Li^b, Ping Su^b, Ling Zhang^b, Kezhen Li^a, Ding Ma^a, Gang Chen^{a,*}, Jing Li^{c,*}, Wenpei Xiang^{b,*}

^a Department of Obstetrics and Gynecology, Tongji Hospital, Tongji Medical College, Huazhong University of Science and Technology, Wuhan 430030, China

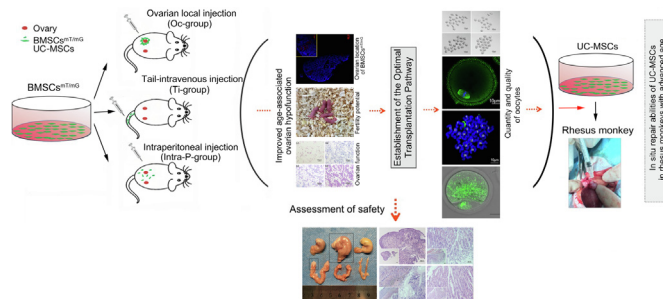
^b Institute of Reproductive Health, Center of Reproductive Medicine, Tongji Medical College, Huazhong University of Science and Technology, Wuhan 430030, China

^c State Key Laboratory of Reproductive Medicine, Nanjing Medical University, Nanjing, Jiangsu, China

HIGHLIGHTS

- Mesenchymal stem cells transplantation (MSCs) to the ovaries of POF patients could lead to effective clinical outcomes.
- Assessment of MSCs effect for single transplantation was performed using 3 transplantation methods.
- MSCs into ovaries by ovarian local injection was determined as the most effective route.
- This technique exerted marked effect on antagonizing age-associated ovarian hypofunction.
- Histopathological data showed that no neoplasms and obvious prosoplasia were found after MSCs transplantation.

GRAPHICAL ABSTRACT



ARTICLE INFO

Article history:

Received 2 June 2021

Revised 1 September 2021

Accepted 3 September 2021

Available online 6 September 2021

Keywords:

Mesenchymal stem cells

Ovarian hypofunction

Natural aging

Oocytes

Mitochondria

Tumorigenicity

ABSTRACT

Introduction: The transplantation of mesenchymal stem cells (MSCs) in patients with premature ovarian failure (POF) could lead to clinical improvement. The transplantation to the ovaries among other transplantation methods have been reported in various animal models, however, there is little evidence regarding the optimal method, including the clinical safety and the efficiency for the treatment of age associated ovarian hypofunction.

Objectives: To establish the most effective transplantation route of MSCs, explore the resistance to therapy, its safety and role in the natural aging process of the ovaries.

Methods: Highly purified MSCs were injected intraperitoneally, directly into the ovaries or tail-intravenously in mice animal model. The ovarian function, quantity and quality of oocytes, cell viability/apoptosis, were evaluated, applying chemiluminescence analysis (CLIA), western blotting, immunofluorescence staining, transmission electron microscope (TEM), TdT mediated dUTP Nick End Labeling (TUNEL) assay and other techniques. The organ tumorigenicity was also evaluated by long-term observation and histopathological examination. The efficiency of MSCs was further verified in non-human primates by the most effective transplantation route.

Peer review under responsibility of Cairo University.

* Corresponding authors.

E-mail addresses: gumpc@126.com (G. Chen), ljwth@njmu.edu.cn (J. Li), wpxiang2010@gmail.com (W. Xiang).

¹ The first two authors contributed to this work.

<https://doi.org/10.1016/j.jare.2021.09.001>

2090-1232/© 2022 The Authors. Published by Elsevier B.V. on behalf of Cairo University.

This is an open access article under the CC BY-NC-ND license (<http://creativecommons.org/licenses/by-nc-nd/4.0/>).

Results: The 32nd week was ultimately determined as the time point of MSCs transplantation. Our results showed that the intra-ovarian injection was the best transplantation method with a more conspicuous effect. With deeper investigations, we found that the transplanted MSCs showed an effective influence on the follicular number, promoted follicle maturation and inhibited cell apoptosis, which was further verified in non-human primates. In addition, the long-term observation and the histopathological examinations ruled out neoplasms or obvious prosoplasia after MSCs transplantation.

Conclusion: MSCs transplantation by intra-ovarian injection could within a month exert the most conspicuous anti-age-associated ovarian hypofunction effects, which may improve the quantity and quality of oocytes by changing the mitochondrial structure, regulating mitochondrial function and attenuating cell apoptosis to increase the storage of the follicle pool without a remarkable potential of tumorigenicity. © 2022 The Authors. Published by Elsevier B.V. on behalf of Cairo University. This is an open access article under the CC BY-NC-ND license (<http://creativecommons.org/licenses/by-nc-nd/4.0/>).

Introduction

A best-established factor, age associated ovarian reserve, is troubling an increasing number of couples who delay childbearing or expect one more child with advanced maternal age [1,2]. Moreover, higher rates of infertility are associated with older age. Clinically, ovarian reserve (generally used to indicate the number and/or quality of oocytes) can be assessed by female age, the antral follicle count (AFC) on ultrasound, the levels of serum anti-Müllerian hormone (AMH), follicle stimulating hormone (FSH) and estradiol (E_2), the clomiphene citrate challenge test, the response to gonadotropin stimulation and oocyte and/or embryo assessment during an ART procedure [3,4].

At birth, approximately 0.7 ~ 2 million primordial follicles are present in the ovaries; however, more than half are lost before puberty, and only ~400 follicles develop into dominant follicles and release oocytes with other follicles ultimately degenerating to atresia during reproductive age [5]. As reports have indicated, decline occurs at an accelerating rate after ~35 years of age for women, and the reduced ovarian reserve with increasing age will result in an imbalanced interaction between hormones, as well as an aberrant quantity and quality of oocytes, eventually leading to the age-related decline in fertility potential [5,6].

Ovarian insufficiency is a loss of ovarian function with a decreasing pregnancy rate; however, it occurs prematurely in some women as imbalanced hormone levels and accelerated ovarian aging due to the influence of environmental and/or social stress, which is also referred to as premature or primary ovarian failure (POF), a condition characterized by hypergonadotropic hypogonadism in women younger than age 40 years [3]. According to the American College of Obstetricians and Gynecologists Committee, the average age at which women give birth is driving by an increasing trend, and female fertility declines gradually but significantly begins approximately at 32 years old [2]. In addition, some reports showed increasing rates of childless women at age > 40 years or at the end of reproductive age in most countries [7,8]; however, whether this finding results from the decline in fertility potential following the postponement of childbearing remains unclear. Clearly, the couples troubled by infertility have gradually increased in recent decades, and age-related infertility appears to have a tendency to increase [9,10]. In addition, a national cohort study conducted in Denmark in 2017 also showed that the total 5-year live birth rates gradually declined from 80% to 26% with advanced fertility age [11]. Thus, it can be seen that the crisis of reproductive aging caused by advanced age cannot be ignored worldwide. Nevertheless, the current routine clinical procedures of assisted reproductive technology (ART) are not of widespread benefit to all female patients with ovarian insufficiency for *in-vitro* fertilization (IVF) treatment, and the embryo/oocyte cryopreservation proposed as a prevention strategy comes with a financial burden and is only appropriate for small number of women of advanced maternal age with high incomes worldwide. To the

moment, a successful therapy for the age-related decline of fertility is lacking. Nevertheless, research is ongoing to identify new ART approaches, which, however, requires long to assess its clinical applicability or a potential pervasive and high-efficiency application, including gene editing technology, artificial gametes (such as the *in-vitro* induction of iPSCs, ESC research), and *in-vitro* activation of follicles (IVA) [12–14].

Irrespective of the safety concerns that must be validated, somatic stem cells (SSCs) therapy has been the focus of considerable research in the field of reproductive medicine. These infusible cell masses with pluripotency were injected into the body via tail intravenous, intraperitoneal and local transplantation and showed a substantial restored potential to improve ovarian function and rescue the long history of infertility in a chemotherapy-damaged mammalian model, which was likely involved in cell proliferation and anti-apoptotic processes through paracrine effect [15–18]. In addition, a breakthrough was achieved in 2018, in which umbilical cord mesenchymal stem cells (UC-MSCs or HuMSCs) in combination with collagen scaffolds could rescue the overall ovarian function in women with POF and result in a successful clinical pregnancy after transplantation [19]. These multipotent stem cells can be easily extracted from different sources, for example; bone marrow mesenchymal stem cells (BMSCs) show several clinical advantages, such as easy access, little immunogenicity, nontumorigenicity and nonethical controversy, and they can be one of the main options for cell therapy.

As previously discussed, mitochondria are extremely enriched in mature oocytes, with a content of approximately 0.15 million copies of mtDNA, the copies of which are more than those in primordial oocytes and most somatic cells in mammals [20]. With more in depth mitochondria-related studies, advanced maternal age was found to be closely associated with mitochondrial dysfunctions in oocytes, mitochondrial swelling, cristae disruption, and reduced ATP and mtDNA copies, which may be responsible for abnormal spindle assembly, chromosome misalignment and nonsegregation, and oocytic aneuploidy, which consequently may reduce the chances of fruitful pregnancy [21]. Furthermore, oocytic maturation is inseparable from the balanced interaction between hormones released by granulosa cells (GCs), which can form the follicular microenvironment and play a key role in oocyte development [22,23]. Previous studies have shown that the changes of GCs in biological function were closely related to the advanced age with imbalanced hormone release, increased apoptosis and impaired mitochondrial function [24–27].

Based on the previous systematic theories and the time limits of the age-related decline of fertility, we hypothesize that the mesenchymal stem cells (MSCs) may have the potential capacity to improve the quality of oocytes and the biological function of GCs, all of which are associated with ovarian function. However, substantially less is known regarding whether the *in-vivo* transplantation of MSCs has a potential effect on resisting ovarian aging and how to maintain oocyte quantity and improve oocyte quality, as

well as the optimal transplantation pathway. Through our study, we aim to establish the most effective transplantation route and identify the effect of MSCs on resisting ovarian hypofunction induced by age, as well as clarify the molecular mechanism of MSCs regulation on ovarian function, to provide a new outlook and strategy for the research on female fertility protection and rescuing ovarian aging, in addition to a guidance for the clinical application and transformation of stem cells.

Materials and methods

Experimental animals

Old female C57BL/6J mice (>4 ~ 5 months, SPF class), young female ROSA^{mt/mG} mice (6 ~ 8 weeks, SPF class) and young male C57BL/6J mice (10 ~ 12 weeks, SPF class) were obtained from the Animal Research Center of Huazhong University of Science and Technology. All mice were adapted for 3 days after their purchase and were maintained under a controlled temperature (26 ± 2 °C) with 12 h (h) light/dark conditions. In addition, the non-human primates (six rhesus monkeys) were bred and supplied by Fujian Experiment Center of Nonhuman Primate for Family Planning, where they were maintained under the first class animal feeding standards (detailed information about these rhesus monkeys are shown in Table S1).

The experiments were approved by the Animal Experimental Ethics Committee of Fujian Provincial Family Planning Institute of Science and Technology in China in accordance with the National Research Council's "Guideline for the Care and Use of Laboratory Animals".

Weeks-old determination of natural aging mice with diminished ovarian function

The mice were divided into seven groups: 16 week-old mice (16w), 20 week-old mice (20w), 24 week-old mice (24w), 28 week-old mice (28w), 32 week-old mice (32w), 36 week-old mice (36w) and 40 week-old mice (40w) (n = 30 per group). Vaginal smears of these mice were obtained to observe the estrus cycle at 08:00 am. The mice with diestrus were selected for serum analysis by inner canthus blood sampling. The obtained blood samples were kept static for 1 h at room temperature (RT), and centrifuged at 3000 rpm for 20 min (min), where the upper serum was then collected for hormone level detection using a CLIA Kit for FSH (CLOUD-CLONE CORP., Ltd), CLIA Kit for Luteinizing Hormone (LH) (CLOUD-CLONE CORP., Ltd), CLIA Kit for AMH (CLOUD-CLONE CORP., Ltd) and CLIA Kit for E₂ (CLOUD-CLONE CORP., Ltd). The remaining mice were allowed to mate with fertile male mice (2:1) for 10 days and checked for fertility.

Chemiluminescence immunoassay (CLIA) detection

Serum samples harvested from the mice of each group were assessed to evaluate the expression levels of E₂, AMH, FSH, and LH according to the guidelines instructions. The serum samples and standards were added into Coated Wells at 50 µl/well, immediately mixed with 50 µl working reagent A and incubated for 1 h at 37 °C with the test plate wrapped with a membrane. The plate was washed and dried 3 times with 350 µl Washing Buffer tautologically, following which 100 µl working reagent B was added, incubated for 30 min at 37 °C, and rinsed five times. Subsequently, 100 µl substrate solution was added into the plate and then incubated for 10 min at 37 °C in the dark with a wrapped membrane. Finally, the chemiluminescence (RLU value) was measured and

recorded by a multifunctional Luminoskan Ascent microplate luminometer.

MSCs isolation, culture and identification

The primary BMSCs^{mt/mG} (Cell membrane-localized strong tdTomato red fluorescence) were isolated and purified from female ROSA^{mt/mG} mice (6 ~ 8 weeks). After the sterile extraction operation of femurs and tibiae, the samples were washed twice in Iscove's Modified Dulbecco Medium (IMDM, GENOM, China). The bone marrow was repeatedly flushed out with complete medium that contained IMDM basal medium, 15% (v/v) fetal bovine serum (FBS, Gibco, USA) and 100 U/ml penicillin-100 mg/ml streptomycin (Gibco, USA), centrifuged at 1000 g for 5 min, resuspended in IMDM complete medium, and cultured in a humidified cell culture incubator (37 °C, 5% CO₂); the culture medium was changed every three days. Adherent cells in passage 4 (P4) identified by flow cytometry (FACS) were characterized by the existence of the typical surface antigens CD29 (Anti-Mouse/Rat CD29 FITC, eBioscience, USA) and CD44 (Anti-Human/Mouse CD44 FITC, eBioscience, USA), as well as the absence of the hematopoietic markers CD34 (Anti-Mouse CD34 FITC, eBioscience, USA) and CD45 (Anti-Mouse CD45 FITC, eBioscience, USA). In addition, osteogenic and adipogenic differentiation was further performed to evaluate the multipotency capability of BMSCs^{mt/mG} in passage 4. The BMSCs^{mt/mG} in fifth passage was used for the subsequent transplantation.

HuMSCs were kindly provided by the Stem Cell Laboratory of the Center of Reproductive Medicine (Tongji Medical College, Huazhong University of Science and Technology, China). Frozen HuMSCs in passage 4 were freshly seeded in 10 cm-culture dishes (1 × 10⁶ cells/dish) in Iscove's modified Dulbecco medium (IMDM, GENOM, China) supplemented with 10% (v/v) fetal bovine serum (FBS, Gibco, USA), 100 U/ml penicillin and 100 mg/ml streptomycin (Gibco, USA). Briefly, the phenotypes of HuMSCs were specifically identified by fluorescence-activated cell sorting (FACS) for the existence of the typical surface antigens CD73 (Anti-Human CD73 PC5.5, eBioscience, USA), CD90 (Anti-Human CD90 PC7, eBioscience, USA), CD105 (Anti-Human CD105 ECD, eBioscience, USA) and CD44 (Anti-Human CD44 PE, eBioscience, USA), as well as the absence of the markers CD34 (Anti-Human CD34 FITC, eBioscience, USA), CD45 (Anti-Human CD45 FITC, eBioscience, USA) and HLA-DR4 (Anti-Human HLA-DR4 FITC, eBioscience, USA), and the osteogenic and adipogenic capacities of the mesenchymal stem cells were assessed with a MesenCult™ osteogenic stimulatory kit (Stemcell Technologies Inc., Canada) and a MesenCult™ adipogenic differentiation kit (Stemcell Technologies Inc., Canada). The fifth passage was used for the experiments.

Osteogenic differentiation of mouse mesenchymal stem cells

MSCs were plated in appropriate complete MesenCult™ medium (1 ~ 2 × 10⁵ cells/ml) and incubated at 37 °C under hypoxic conditions until they were approximately 80 ~ 90% confluent; the medium was aspirated and replaced with complete MesenCult™ Osteogenic Medium that contained the MesenCult™ MSC Basal Medium (STEMCELL Technologies Inc. Canada) and 20% MesenCult™ Osteogenic Stimulatory Supplement (STEMCELL Technologies Inc. Canada). The cells were then continuously incubated at 37 °C in hypoxic conditions until bone matrix formation was observed. After aspirating the medium the cells were fixed in 4% paraformaldehyde for 15 min rinsed three times with PBS and stained with Alizarin Red S solution (Sigma-Aldrich Merck USA) for 5 ~ 10 min at RT to assess the calcium deposits and the quantitative analyses of calcification

Adipogenic differentiation of mouse mesenchymal stem cells

MSCs were plated in appropriate complete MesenCult™ medium ($1 \sim 2 \times 10^5$ cells/ml) and incubated at 37 °C under hypoxic conditions until they were approximately > 90% confluent; the medium was aspirated and replaced with complete MesenCult™ Adipogenic Medium (MesenCult™ MSC Basal Medium + 10 %10 × MesenCult™ Adipogenic Differentiation Supplement + 2 mM L-Glutamine STEMCELL Technologies Inc. Canada). The cells were then continuously incubated at 37 °C in hypoxic conditions until lipid droplets were observed. After aspirating the medium the cells were fixed in 4% paraformaldehyde for 15 min rinsed three times with PBS and stained with Oil Red O solution (Sigma-Aldrich Merck USA) for 8–10 min at RT to detect and quantify the lipid droplet formation

MSCs transplantation

Mice of 32 weeks-old were randomly divided into three equal groups: Oc + BMSCs group (ovarian local injection), Ti + BMSCs group (tail-intravenous injection) and Intra-P + BMSCs group (intra-peritoneal injection), all the above were injected with normal saline (NS) as control groups. As previously described [28,29], all of the mice were appropriately transplanted with a concentration of 1.2×10^7 /ml MSCs (6×10^5 MSCs in 50 µl normal saline) by intraperitoneal, intravenous or ovarian local injections, respectively.

Comparison of the ovarian follicle count

Serial paraffin sections were created from the ovarian tissues after MSCs transplantation, and a slice was obtained at every five intervals for staining with H&E. All stages of follicles (primordial, primary, secondary, antral follicles and atretic follicles) were detected and classified. The number of follicles from each ovary was calculated and compared between each group (n = 5, per group).

Western blotting analysis

Proteins (40 µg) were separated by SDS-PAGE and transferred to 0.45 µm PVDF membranes. Nonspecific binding was blocked with 5% nonfat milk for 1 h at RT. The membranes were hybridized with rabbit monoclonal [NIAR164] to Mfn2 antibody (Abcam, USA), rabbit polyclonal anti-Mfn1 antibody (Abcam, USA), rabbit polyclonal anti-OPA1 antibody (Abcam, USA), rabbit polyclonal anti-DRP1 antibody (Abcam, USA), rabbit polyclonal anti-Bcl-2 antibody (Cell Signaling, USA), rabbit polyclonal anti-Bax antibody (Cell Signaling, USA), rabbit polyclonal anti-caspase3 antibody (Cell Signaling, USA), rabbit polyclonal anti-caspase9 antibody (Cell Signaling, USA), rabbit monoclonal anti-Foxo3a antibody (Cell Signaling, USA), rabbit polyclonal anti-P-PI3K antibody (Boster Biological Technology Co. Ltd, USA), rabbit polyclonal anti-P-AKT antibody (Affinity Biosciences, Inc., USA), rabbit polyclonal anti-β-actin antibody (Santa Cruz Biotech, CA) and rabbit polyclonal anti-COX IV antibody (Abcam, USA) in TBST that contained 1% nonfat milk overnight. The membranes were washed with TBST four times, each time for 10 min, followed by incubation with goat anti-rabbit horseradish peroxidase (HRP)-conjugated secondary antibody (Invitrogen, USA) at 37 °C for 1 h. After four washes in TBST, immunoreactive bands were visualized by an enhanced chemoluminescent system (P1108, Beyotime Institute of Biotechnology, China). The band intensity was quantified by densitometry using Quantity One 4.6.9 analysis software (Bio-Rad, USA). The results were normalized to the β-actin or COX IV signal intensity.

Immunofluorescence staining

Frozen sections (8–10 µm) from ovarian tissues were rewarmed and fixed for 15 mins in 4% paraformaldehyde (PFA, Sigma, USA) at RT. Following antigen retrieval, a nonspecific staining was sealed with 5% bovine serum albumin (BSA, Sigma, USA) and 0.3% Triton X-100 at RT for 1 h. Immunocytochemical analysis was also used to verify the intracellular localization of FOXO3a in oocytes and cumulus granulosa cells. The slides or fixed cells were incubated overnight at 4 °C with anti-tdTomato antibody (1:100, Abcam, USA) or anti-Foxo3a antibody (1:500, Cell Signaling, USA), and PBS was used as a negative control instead of the primary antibody for each section. After rinsing three times with PBS for 5 min, the slides were incubated with the Goat Anti-Rabbit IgG H&L (Alexa Fluor® 647 or Alexa Fluor® 488) (Abcam, USA) for 60 min at RT and then counterstained with DAPI (Boster, Wuhan) for 5 mins after PBS washing; the slides were covered with ProLong™Gold anti-fade reagent (Servicebio, Wuhan) and analyzed under a fluorescence microscope. Both groups were processed under identical conditions.

Transmission electron microscopy (TEM)

Fresh ovarian tissues ($1 \times 1 \times 1$ mm³) were immersed in cryogenic fixed liquid (Servicebio, China) for 2 ~ 4 h at 4 °C after being washed with fixed liquid that contained 2.5% glutaraldehyde and were then immediately sent to the ultrastructural pathological room of Wuhan Institute of Virology, CAS for subsequent operation. The ultrastructure was observed using a 200 kw transmission electron microscope (FEI, Tecnai G20 TWIN, USA).

TUNEL assay

A terminal deoxynucleotidyl transferase-mediated dUTP nick end labeling (TUNEL) assay was employed using the In Situ Cell Death Detection Kit (Roche, Sigma-Aldrich, USA). For 4 µm-thick paraffin sections, the slices were dewaxed and rehydrated according to standard protocols, and the sections were then rinsed twice with distilled water for 2 min. After the addition of 50 µl Protein K working solution ($1 \times$) to the paraffin sections and incubation for 25 min at 37 °C, the slices were rinsed three times with distilled water; intraprep permeabilization reagent (Servicebio, China) was added to the samples for 20 min at RT, and the samples were rinsed three times, followed by the addition of TUNEL reaction mixture that contained TdT and dUTP (1:9) to the sample, incubation at 37 °C for 2 h in a humidified atmosphere, and rinsing with PBS three times. Finally, the samples were counterstained with DAPI and analyzed under a fluorescence microscope. The apoptosis index (AI) was analyzed by Image-Pro Plus 6.0 software and calculated as $AI = (\text{No. of TUNEL-positive nuclei in one zone}) / (\text{No. of total nuclei in the same zone}) \times 100\%$.

Mitochondrial membrane potential ($\Delta\Psi_m$) detection

The membrane potential of mitochondria was observed by fluorescence microscopy after detection by the JC-1 Mitochondrial Membrane Potential Assay Kit (Beyotime, China). The ovarian tissues were rinsed, cut up, drawn with a pipettor, filtered with a 200 mesh sieve, and then centrifuged at 1000 rpm for 5 mins to remove cell debris. The cell precipitate resuspended in 500 µl complete culture medium was incubated with 500 µl JC-1 fluorescent dye in a 5% CO₂ incubator for 30 min at 37 °C and then centrifuged and washed slowly with JC-1 working liquid three times. The mitochondrial membrane potential was analyzed by a fluorescence microscope with the green signal of JC-1 measured at 485/535 nm and the red signal measured at 590/610 nm.

Total DNA extraction and the quantification of mtDNA (copies)

Total DNA was extracted from ovarian tissues using TIANamp Genomic DNA Kits from TIANGEN (TIANGEN BIOTECH CO., LTD, BEIJING) according to the manufacturer's protocol. Five microliters total DNA (100 ng/ μ l) was dissolved in 20 μ l PCR mixtures according to the All-in-One qPCR Mix Kit (Genecopoeia, USA), and the mtDNA content was assessed by the quantification of the mitochondria-specific *ND-1* gene relative to the nuclear gene β -actin. The *ND-1* primer sequences were as follows: Forward 5'-TA CTTCTGCCAGCCTGACC-3' and Reverse 5'-CGGCTGCGTATTC TACGTT-3'. The β -actin primer sequences were as follows: Forward 5'-GTCCCTCACCTCCCAAAG-3' and Reverse 5'-GCTGCCTCAA CACCTCAACCC-3'. SYBR Green three-step quantitative real-time polymerase chain reaction (RT-qPCR) was performed in triplicate by an MX3000P Real-Time PCR Detection System (Stratagene, USA), and the amplified transcripts were normalized to the β -actin expression using the comparative Ct method. Briefly, the Ct values were calculated according to the following equation: $\Delta Ct = Ct_{ND-1} - Ct_{\beta-actin}$; the relative quantity of mtDNA expression in the BMSC-graft groups was then compared with the control groups. The final copies were calculated by the following formula: $X_n = 2^{-\Delta\Delta Ct}$.

Oocyte microtubulin immunofluorescence staining (spindle detection)

M II Oocytes were obtained, denuded with hyaluronidase (Sigma, USA), fixed in 4% PFA at RT for 30 min and then permeabilized with 0.1% Triton X-100 for 20 min. After blocking in 3% BSA supplemented with phosphate-buffered saline (PBS) for 1 h, the samples were incubated overnight at 4 °C with anti- α -tubulin monoclonal antibody (1:100, Proteintech Group, Inc., China). After being rinsed three times in PBS, the oocytes were incubated with 1:100 Alexa Fluor488-conjugated Affinipure Goat Anti Mouse IgG (1:100, Proteintech Group, Inc., China) protected from light at 37 °C for 1 h, redyed for nuclear imaging with DAPI for 5 min in the dark, and then observed with a confocal microscope (IX71, Olympus, Japan).

Mitochondrial distribution

Oocytes (M II) and GCs were collected and cultured in 0.4 μ M/L Mito-Tracker Green (1 mM supplemented with 3% BSA, Beyotime Institute of Biotechnology, China) for 30 min at 37 °C in a humidified atmosphere with 5% CO₂. After washing three times, the oocytes and GCs were analyzed using a confocal microscope (IX71, Olympus, Japan).

Chromosome aneuploidy detection

For chromosomal spread, oocytes (M II) were incubated in acid Tyrode's solution (Sigma, USA) to remove the zona pellucida. After washing three times in M2 medium, the oocytes were transferred onto a glass slide and fixed with 1% paraformaldehyde, 0.15% Triton X-100 and 3 mmol/L dithiothreitol in distilled water at RT. After drying in air, the slides were blocked in PBS that contained 1% BSA at room temperature for 1 h, incubated with primary antibodies (1:100) overnight at 4 °C, and then washed three times and incubated with secondary antibody at room temperature for 2 h. Finally, the chromosomes were stained with DAPI, and the slides were viewed via immunofluorescence microscopy.

Ethics statement

All experiments involving animals were conducted according to the ethical policies and procedures approved by the Animal Experimental Ethics Committee of Fujian Provincial Family Planning Institute of Science and Technology in China (Approval no. 2018-03) and the Institutional Animal Care and Use Committee at Tongji Medical College of Huazhong University of Science and Technology in China (Approval no. S510).

Statistical analysis

Each experiment was repeated more than three times with consistent results, and the data, presented as the mean \pm SD, were analyzed with SPSS Statistics 17.0. Statistical significance. The normally distributed numerical variance was performed by two-way ANOVA with homogeneity of variance, and Chi Square tests (χ^2 test) were employed for the differences between two or more rates. In addition, we collected three technical replicates from each nonhuman primate experiment. The statistical significance was set at $P < 0.05$.

Results

Determination of the appropriate mouse-age for MSCs transplantation

To determine the appropriate age for transplantation, we distributed these mice into seven groups: 16 weeks old (16w), 20 weeks old (20w), 24 weeks old (24w), 28 weeks old (28w), 32 weeks old (32w), 36 weeks old (36w) and 40 weeks old (40w) ($n = 30$, per group). We observed the pregnancy and average litter size of the mice and collected the serum at the same menstrual cycle of each group for the FSH, LH, E₂ and AMH level detection, respectively. The results showed that both the pregnancy rate (Fig. S1A) and the average litter size (Fig. S1B) were markedly declined at 28w ($P < 0.05$).

Moreover, the hormone levels in each group were detected; the CLIA assay demonstrated the serum AMH level (Fig. S1C) and E₂ (Fig. S1D) level gradually decreased with the increased age and significantly decreased at 28w and 32w, respectively ($P < 0.01$). The levels of FSH (Fig. S1E) and LH (Fig. S1F) at different observed weeks gradually increased with age, and both levels were significantly increased at 32w ($P < 0.01$). According to these results, mice of 32 weeks were ultimately determined to be the appropriate mouse-age for MSCs transplantation.

BMSCs^{mT/mG} and UC-MSCs phenotype characterization and pluripotency assessment

BMSCs^{mT/mG} were isolated from female ROSA^{mT/mG} mouse bone marrow of the tibia and femur, which appeared similar to the typical spindle-shaped fibroblast-like cells and showed intrinsic cell membrane-localized tdTomato (mT) fluorescence after several generations of cultivation (Fig. S2A). The adherent and homogeneous cell population was identified by FACS after three passages. The immunophenotypes of the mesenchymal and hematopoietic marker expressions in passage 4 were analyzed. The results showed that the mesenchymal markers with CD29 (99.9%) and CD44 (97.0%) were positive and the hematopoietic cell surface markers CD34 (1.9%) and CD45 (1.2%) were negative (Fig. S2B). The *in-vitro* differentiation potential of BMSCs^{mT/mG} was assessed. In mesenCult™ adipogenic differentiation medium, the BMSCs^{mT/mG} were stimulated for 21 days, and lipid droplets were diffusely present in the cytoplasm after Oil Red O staining (Fig. S2C, a ~ d). The osteogenic differentiation potential of BMSCs^{mT/mG}

was detected with alizarin red staining, and the result showed that it was positive by the presence of calcium deposition after 21 days of stimulation (Fig. S2C, $e \sim h$). These findings indicated that the BMSCs^{mT/mG} in passage 5 can be appropriate for transplantation due to the high degree of purification.

UC-MSCs in passage 4 had an appearance that was similar to typical spindle-shaped fibroblast-like cells, and they were arranged closely with vortex-like growth, the fluorescent-activated cell sorting (FACS) showed that the targeted cells expressed CD44 (99.79%), CD73 (99.46%), CD90 (99.74%), and CD105 (99.91%), but not CD34, CD45 and HLA-DR (<1%; Supplementary Fig. S3A). The positive cells expanded in the enriching culture were successfully induced to become osteoblasts with bone matrix formation and adipocytes with lipid droplet formation (Fig. S3B).

Assessment of the animal model: Establishment of the optimal transplantation pathway

Subhead 1: In-vivo effect of transplanted BMSCs^{mT/mG} in the three injection methods and more sensitive effect in Oc+ and Ti + BMSCs groups

By preliminary comparison of the three transplantation methods, the hormone levels in the serum were detected after BMSCs^{mT/mG} transplantation for four weeks. The transplanted BMSCs^{mT/mG} exerted a more sensitive effect on the upward trends about AMH and E₂ levels and downward trends about FSH levels in the Oc + BMSCs group and Ti + BMSCs group compared with those in the Intra-P + BMSCs group, with significant rising about AMH levels in Oc + BMSCs compared with that in Intra-P + BMSCs ($P < 0.01$, Fig. 1A). Furthermore, follicles with HE-staining in each stage were shown in the Oc-, Ti- and Intra-P + BMSCs groups (Fig. 1B). When compared to the Intra-P + BMSCs, the numbers of primordial follicles (21.00 ± 6.38 vs. 5.60 ± 1.50 , $P < 0.01$), primary follicles (22.67 ± 6.02 vs. 6.20 ± 1.16 , $P < 0.01$), secondary follicles (17.00 ± 5.72 vs. 11.80 ± 1.94 , $P < 0.05$) were significantly increased after transplantation for four weeks in the Oc + BMSCs with slightly increased levels in Ti + BMSCs group just for primordial follicles (11.60 ± 3.61 vs. 5.60 ± 1.50 ; $P < 0.05$). Ultimately, the Oc + and Ti + BMSCs groups were selected for further assessment.

Subhead 2: Ovarian location of transplanted BMSCs^{mT/mG} in Ti + and Oc + BMSCs groups

The immunofluorescence analysis tracked the ovarian location of transplanted BMSCs^{mT/mG}, and the results indicated the homing to ovaries after transplantation for four (36 weeks old, 36w) and eight weeks (40 weeks old, 40w). The red staining (anti-tomato) cells were defined as BMSCs^{mT/mG} (Fig. S4). BMSCs^{mT/mG} were scattered and randomly distributed in the ovarian tissue without developing into follicles, even after transplantation for eight weeks by the tail intravenous injection and ovarian local injection. However, compared with the 36w mice, the amount of transplanted BMSCs^{mT/mG} in the 40w mice was basically decreased without obvious proliferation. In addition, the transplanted BMSCs^{mT/mG} were not detected in the control group.

Subhead 3: In vivo effect of BMSCs^{mT/mG} on the declined ovarian function induced by age and conspicuous effect in Oc + BMSCs group

The evaluation of the mouse estrous cycle at two months after BMSCs^{mT/mG} transplantation by tail-intravenous and ovarian local injection (Fig. 2A, Fig. 2B) revealed that BMSCs^{mT/mG} in the Oc + BMSCs or Ti + BMSCs group could increase the number of estrous cycles compared with the Oc + NS group ($P < 0.001$) or Ti + NS group ($P < 0.01$), respectively; However, compared with the Ti + BMSCs group, the Oc + BMSCs group showed a more pronounced increase (9.25 ± 0.96 vs. 7.9 ± 0.83 , $P < 0.001$) (Fig. 2C). Moreover, the percentage of mice with normal estrous cycle was

also increased after four weeks of BMSCs^{mT/mG} transplantation, and in particular, the Oc + BMSCs group exhibited a conspicuous effect (Fig. 2D; Table S2, $P < 0.01$). Compared with the Ti + BMSCs group, the method of ovarian local injection was more effective at 37w–38w (100% vs. 80.0%) and 39w–40w (88.2% vs. 60.0%) (Fig. 2D; Table S2). In addition, the average duration of estrus was significantly prolonged in the BMSCs^{mT/mG}-transplantation groups, particularly for the durative days in the Oc + BMSCs group compared with that in the Oc + NS group at 37w–38w (2.00 ± 0.58 vs. 1.00 ± 0.88 , $P < 0.05$) and 39w–40w (2.24 ± 1.16 vs. 0.93 ± 0.83 , $P < 0.05$); moreover, the results in the Oc + BMSCs group also showed a remarkable difference at 37w–38w (2.0 ± 0.58 vs. 0.78 ± 1.09 , $P < 0.05$) and 39w–40w (2.24 ± 1.16 vs. 0.38 ± 0.74 , $P < 0.01$) compared to those in the Ti + BMSCs group (Fig. 2E; Table S3/4/5/6), and proestrus or diestrus decreased in their duration.

Nevertheless, the ovarian tissues were extracted, and the weights were measured. The results showed that these ovaries had a ruddy and normal appearance with some follicle protuberances on the surface (Fig. 2F). In the Ti + BMSCs group, the ovarian tissues were enlarged in size after eight weeks of BMSCs^{mT/mG} transplantation (40w) compared to that in the Ti + NS group without a significant change in size at 36w, and the weight index of the ovaries (ovarian weight/mouse weight) also showed the same increasing tendency (Fig. 2F). By comparison, BMSCs^{mT/mG} exhibited a conspicuous effect in the Oc + BMSCs group with a clear enlargement in size after four weeks of BMSCs^{mT/mG} transplantation (36w) and a significant difference in the weight index, particularly at 40w ($P < 0.01$) (Fig. 2G). The steroid hormones in the serum were detected after BMSCs^{mT/mG} transplantation. The CLIA test demonstrated that the levels of FSH (declined as much as 15.5%) and LH (declined as much as 22.7%, $P < 0.05$) in the Ti + BMSCs group were slightly rescued by BMSCs^{mT/mG}, and both the AMH and E₂ levels maintained an upward trend in the Ti + BMSCs group compared to those in the Ti + NS group (Fig. 2H). However, in comparison, the levels of FSH significantly decreased up to 17.6% ($P < 0.05$), and LH remarkably decreased up to 27.3% ($P < 0.01$). Moreover, the AMH and E₂ levels showed significant increases up to 24.8% ($P < 0.05$) and 29.0% ($P < 0.05$).

Subhead 4: In-vivo effect of BMSCs^{mT/mG} on fertility potential and conspicuous effect in the Oc + BMSCs group

At the third day of BMSCs^{mT/mG} injection, the female mice of each group were housed with proven fertile males for 10 days at a ratio of 1:2 for mating trials. The number of offspring per litter and pregnant mice were subsequently recorded (Fig. S5A). All measured outcomes indicated that BMSCs^{mT/mG} transplantation into mice could improve the reproductive capability, including the pregnancy rate and the average litter size per pregnancy. Compared with the Ti + NS and Oc + NS groups, respectively, both the rate of pregnancy (Fig. S5B; Table S7) and the average litter size (Fig. S5C; Table S8) showed escalating trends in the Ti + BMSCs and Oc + BMSCs groups, and the effect in the Oc + BMSCs group was more conspicuous.

Preliminary assessment of safety for BMSCs^{mT/mG} transplantation in vivo

To further evaluate the potential for abnormal differentiation of BMSCs^{mT/mG} after transplantation for long-term retention *in vivo*, long-term observation and histopathological data showed that no neoplasms were detected six months to one year after transplantation. Prosoplasia with fibrous hyperplasia, decreased macrophages, increased cell proliferation and inflammatory response were (Fig. S6A/B). In addition, when compared with the control group,

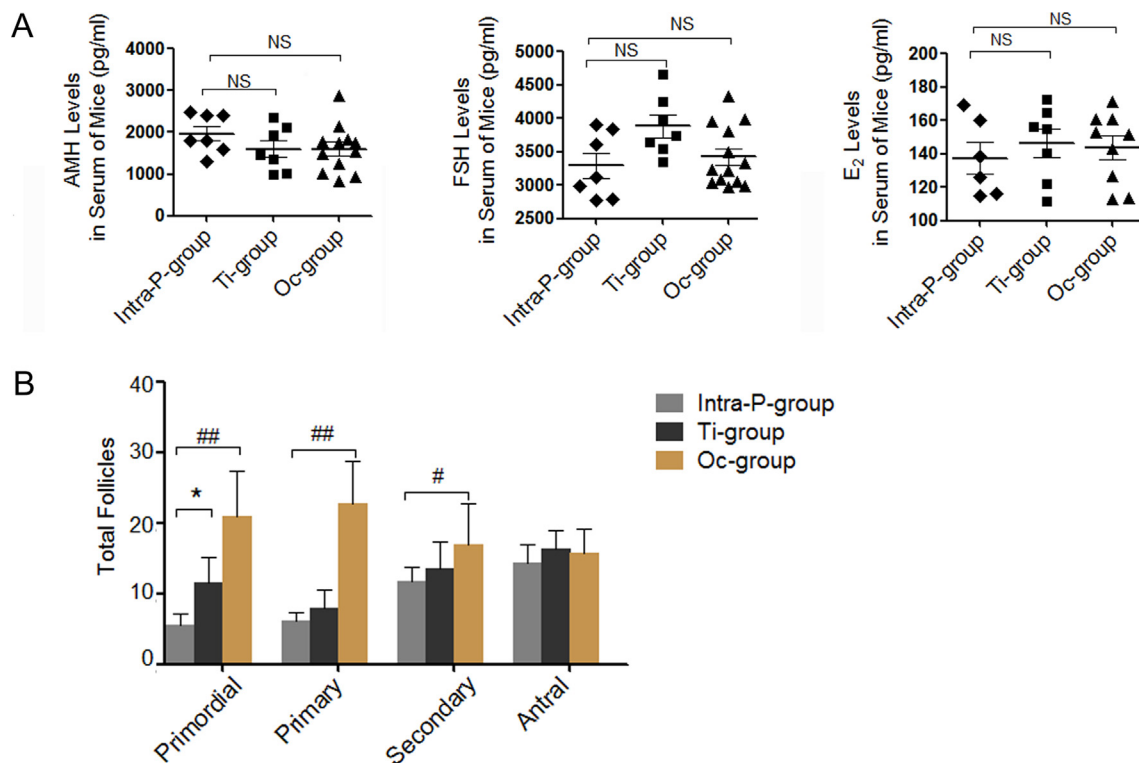


Fig. 1. In vivo effect of transplanted BMSCs^{MT/mG} in the three injection methods. **A** The hormone levels of FSH/AMH/E₂ were measured by CLIA test at 36w. **B** The numbers of primordial follicles, primary follicles, secondary follicles and antral follicles, The error bars indicate SD. * $P < 0.05$, ** $P < 0.01$, *** $P < 0.001$ vs. Intra-P + BMSCs. NS: no statistical differences (vs. Intra-P + BMSCs).

the rate of natural death decreased observably, but without significant difference of the rate of abnormality (Fig. S6C; Table S9).

BMSCs^{MT/mG} increased the follicle number in Oc + BMSCs group 4 weeks after transplantation

The optimal transplantation route, BMSCs^{MT/mG} were injected into the ovary, the follicles with HE-staining in each stage in the Oc + BMSCs group and the control group (Oc + NS) were analyzed after transplantation four/six/eight weeks, (Fig. 3A). The numbers of primordial follicles, primary follicles and secondary follicles were significantly increased after transplantation for four weeks in the Oc + BMSCs group compared with those in the Oc + NS group (21.00 ± 7.81 vs. 6.67 ± 3.79 ; 22.67 ± 7.37 vs. 7.00 ± 1.00 ; 17.00 ± 2.00 vs. 11.00 ± 2.65 ; $P < 0.05$); however, there was no significant difference after transplantation for eight weeks (Fig. 3B/C/D). Nevertheless, the number of antral follicles markedly increased with the duration of BMSCs^{MT/mG} therapy ($P < 0.05$), even at 40w after BMSCs^{MT/mG} transplantation for eight weeks (7.57 ± 1.59 vs. 3.75 vs. 0.83 , $P < 0.01$, Fig. 3E). In addition, we found that the antral follicle count substantially decreased with the duration of BMSCs^{MT/mG} treatment compared to the control group (26.00 ± 5.76 vs. 42.75 ± 4.02 , $P < 0.01$, Fig. 3F).

BMSCs^{MT/mG} improved oocyte quality in Oc + BMSCs group of natural aging mice

After BMSCs^{MT/mG} were administered via ovarian local injection for four and eight weeks, the MII stage oocytes were obtained for *in vitro* fertilization (IVF) and developed to 2-cell stage zygotes and blastocysts. The results indicated that BMSCs^{MT/mG} transplantation affected the fertilization and cleavage of oocytes. The early embryo formation rate in the Oc + BMSCs group (75%, 69%, 64%,

and 55%) was substantially increased compared with that in the Oc + NS group (61%, 54%, 48%, and 34%) at 36w after BMSCs^{MT/mG} transplantation (Fig. 3G, Fig. 3H; Table S10).

To explore the underlying mechanisms of the effect of BMSCs^{MT/mG} on oocytes' developmental potential, we investigated the spindle assembly and chromosome arrangement. We observed aberrant changes in the spindle apparatus, as well as chromosome alignment and separation in the Oc + NS group, such as spindles with abnormal polarization and disordered microtubules (Fig. 3I, b/c), misalignment chromosome (Fig. 3I, b/c) and the homologous chromosome without separation despite the first polar body education (Fig. 3I, d). Distinctly, compared to the Oc + NS group, the transplanted BMSCs^{MT/mG} could ameliorate the abnormal situation with declined disordered spindle assembly (51.06% vs. 70.83%, $P < 0.05$, Fig. 3J; Table S11) and the decreased percentage of aneuploid arrested at the MII stage with 18 or 21 sister chromatids (20.37% vs. 39.13%, $P < 0.05$, Fig. 3K/L; Table S12). BMSCs^{MT/mG} reversed the poor developmental potential and arrested meiosis of oocytes.

MSCs changed oocytes mitochondrial distribution and enhanced ovarian mitochondrial function

To further confirm the underlying mechanisms of transplanted MSCs on oocytes in mice, we observed the mitochondrial redistribution of oocytes at the MII stage with a normal polarity distribution around the spindle. Our results showed that there were three patterns of mitochondrial distribution in the Oc + NS group, including polarity, homogeneous distribution and heterogeneous clusters (Fig. 4A). Surprisingly, in the Oc + BMSCs group, the normal polarity distribution of mitochondria was apparently increased compared to the Oc + NS group (57.14% vs. 35.42%, $P < 0.05$), while

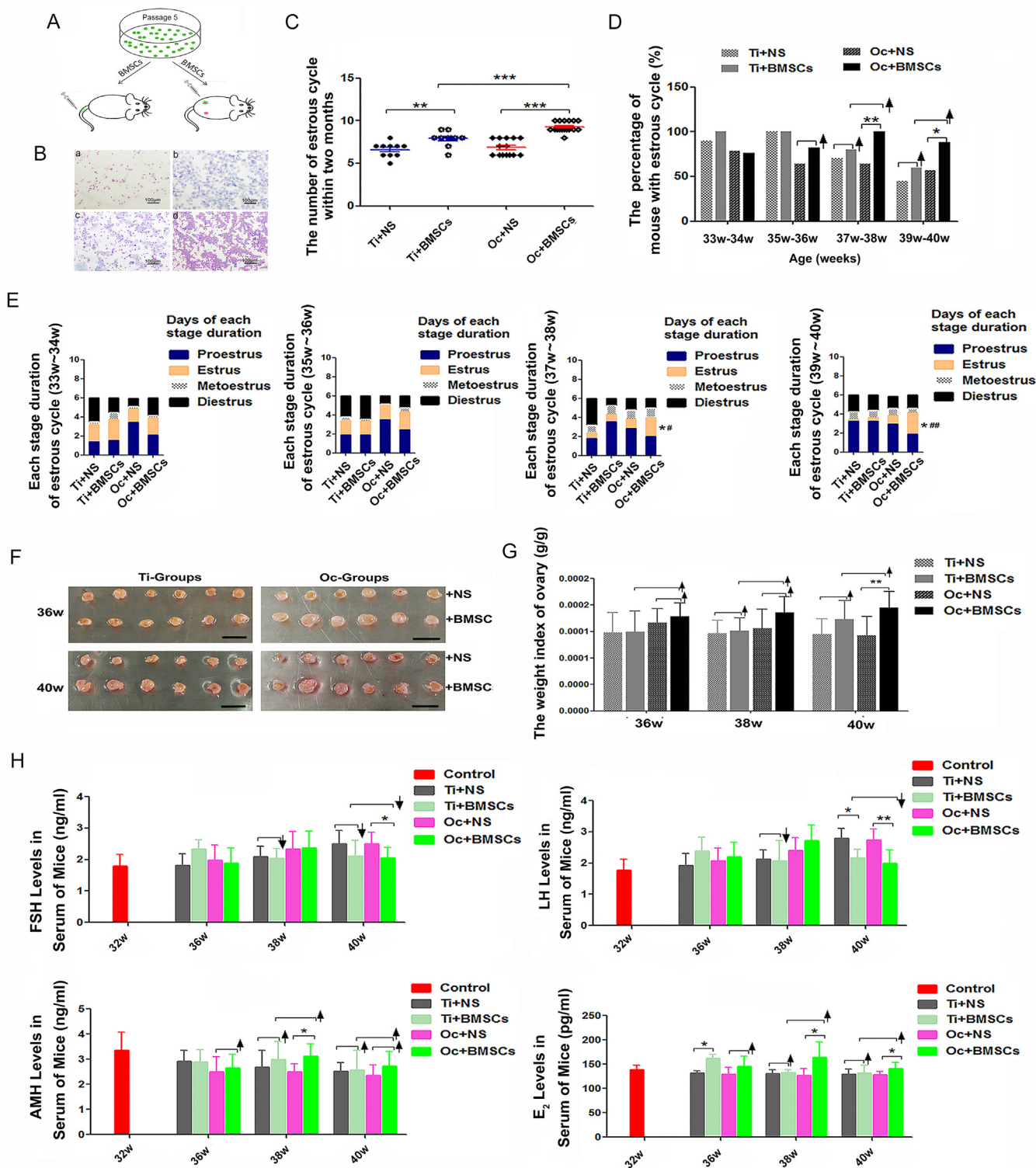


Fig. 2. The consecutive two-month evaluation of the mouse estrous cycle, ovarian morphology and hormone levels after BMSCs^{MT/mG} transplantation. **A** An ideograph of BMSCs^{MT/mG} transplantation by tail intravenous and ovarian local injection. **B** Representative images of the estrous cycle: a: Proestrus; b: Estrus; c: Metoestrus; d: Diestrus. Scale bar = 100 μm. **C** The number of estrous cycles between the four groups within two months. ***P* < 0.05, ****P* < 0.001. **D** The percent of mice with an estrous cycle at more than one time point. **P* < 0.05, ***P* < 0.01, † shows rising tendency from control groups; **E** Each stage duration of estrous cycle between the four groups; the estrous cycle decreasing with age was increased and prolonged due to BMSCs^{MT/mG}. *Significantly different from Oc + NS at *P* < 0.05, #Significantly different from Ti + BMSCs at *P* < 0.05, ##Significantly different from Ti + BMSCs at *P* < 0.01. **F** Ovaries from 36w and 40w mice after four and eight weeks of BMSCs^{MT/mG} transplantation. Isolated ovaries for Ti + BMSCs vs. Ti + NS and Oc + BMSCs vs. Oc + NS. Scale bar = 10 mm; **G** The weight index of ovaries isolated from 36w, 38w and 40w mice in Ti + NS, Ti + BMSCs, Oc + NS and Oc + BMSCs groups. **H** The hormone levels of FSH/LH/AMH/E₂ were measured by CLIA test at 32w, 36w, 38w and 40w of each group. The error bars indicate SD. **P* < 0.05; ***P* < 0.01; † shows rising tendency; ‡ shows downtrend.

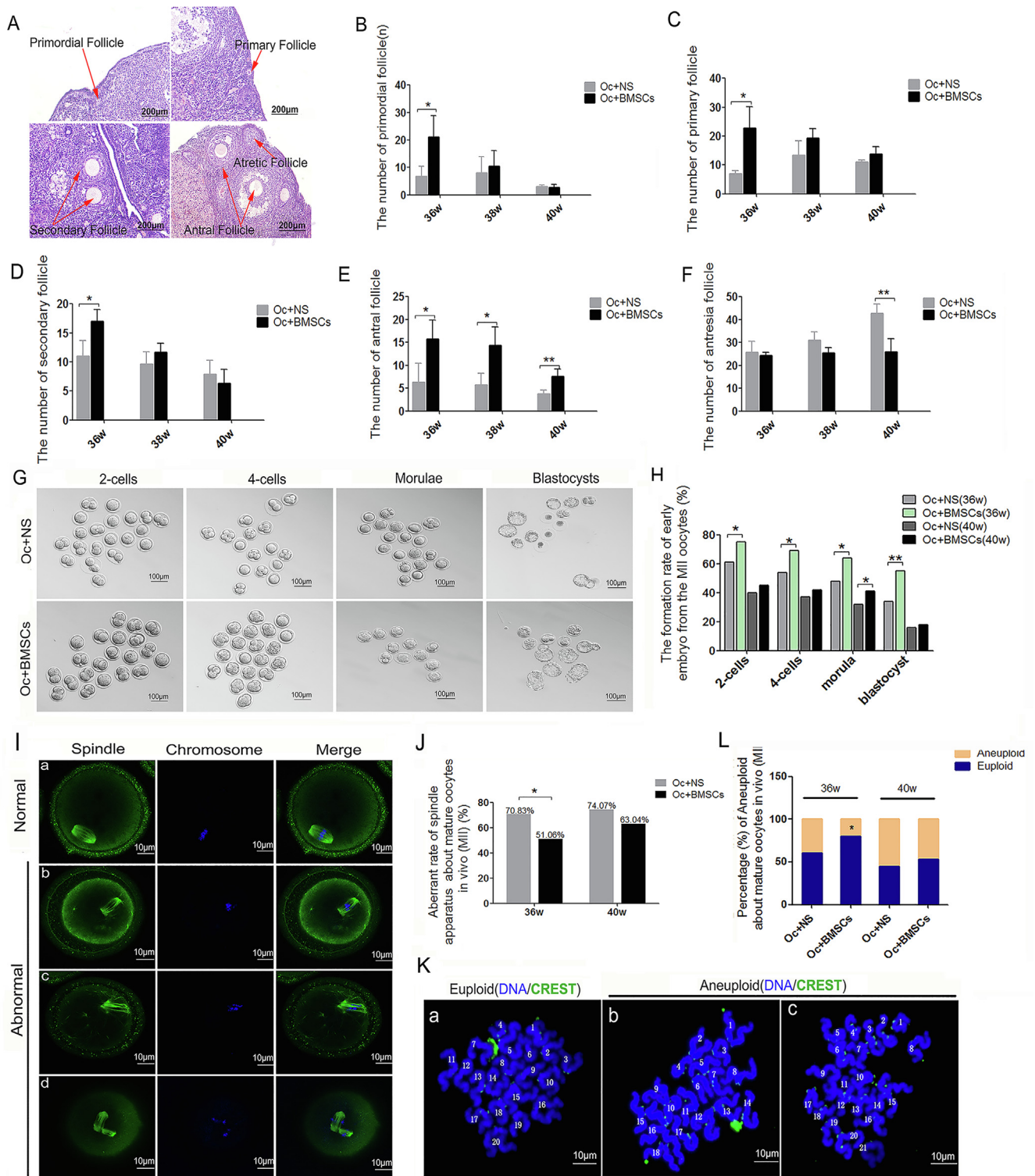


Fig. 3. The effect of transplanted BMSCs^{mt/mg} on follicle development and maturation, as well as the oocyte development and meiosis. **A** Representative images of follicular morphology in each stage with HE-staining. Scale bar = 200 μ m. **B** The number of primordial follicles. **C** The number of primary follicles. **D** The number of secondary follicles. **E** The number of antral follicles. **F** The number of antrisia follicles. * $P < 0.05$; ** $P < 0.01$. **G** The comparative image of 2-cells, 4-cells, morulae and blastocysts in Oc + NS and Oc + BMSCs groups. Scale bar = 100 μ m. **H** Formation rate of the early embryos from MII oocytes after fertilization at 36w and 40w of mice in Oc + NS and Oc + BMSCs groups. **I** Confocal microscopy images of spindles and chromosome of oocytes (MII), Scale bar = 10 μ m; a: Normal spindle assembly and chromosome arrangement; b/c/d: Abnormal spindle assembly and chromosome arrangement. **J** Aberrant rate of spindle apparatus about oocytes (MII) at 36w and 40w of mice in Oc + NS and Oc + BMSCs groups. **K** Representative chromosome spreads from oocytes (MII) are shown by immunofluorescence for DNA (DAPI, blue) and CREST (green), Scale bar = 10 μ m; a: Representative image of euploidy with 20 sister chromatids; b/c: Representative image of aneuploidy with 18 or 21 sister chromatids. **L** Percentage (%) of aneuploidy about mature oocytes (MII) at 36w and 40w of mice in Oc + NS and Oc + BMSCs groups. * $P < 0.05$; ** $P < 0.01$.

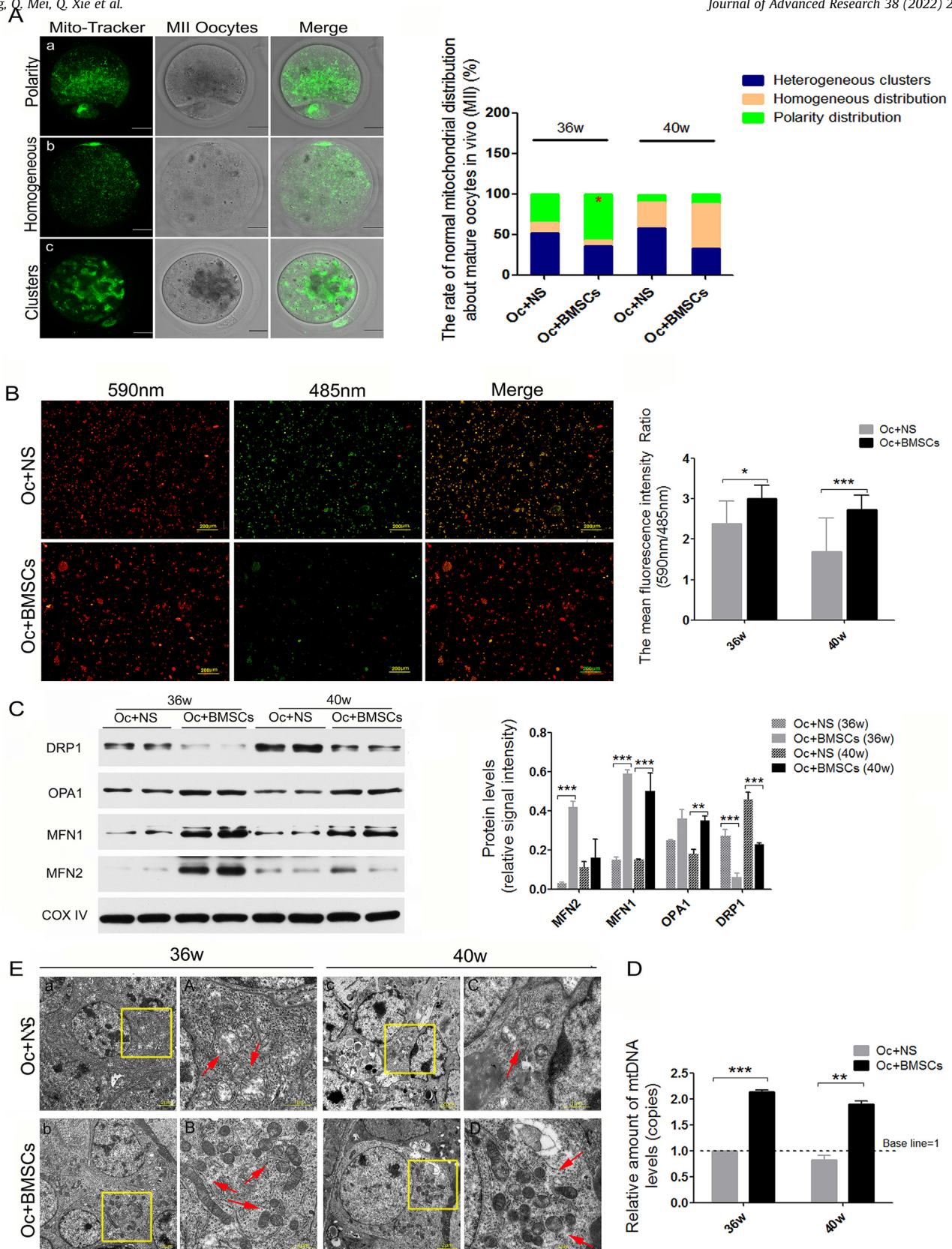


Fig. 4. The changes in mitochondrial structure and function after MSCs transplantation in Oc + NS and Oc + BMSCs groups. **A** Representative images of mitochondrial distribution of MII oocytes with Mito-Tracker Green staining; a: Polarity distribution; b: Homogeneous distribution; c: Heterogeneous clusters; Scale bar = 10 μm; The rate of normal mitochondrial distribution about MII oocytes at 36 and 40w after MSCs injection in Oc + NS and Oc + BMSCs groups. **B** The mitochondrial membrane potential ($\Delta\Psi_m$) of ovaries from the two groups, tested by JC-1. Scale bar = 200 μm; The mean fluorescence intensity ratio (590 nm/485 nm), according to JC-1 staining. **C** The most representative image of mitochondrial dynamics-related protein expression level by western blotting and the relative signal intensity of mitochondrial dynamics-related protein levels. **D** Relative amount of mtDNA copy levels. **E** Representative image of mitochondrial ultrastructure detected by TEM [a ~ d: the most representative mitochondrial morphology from the granulosa cells around oocyte, Scale bar = 2 μm; A ~ D: higher magnification of mitochondria (red arrow) from the yellow frame, Scale bar = 1 μm]. * $P < 0.05$, ** $P < 0.01$, *** $P < 0.001$ vs. the Oc + NS group.

the pattern of heterogeneous clusters and homogeneous distribution were decreased (Fig. 4A; Table S13).

Mitochondrial dysfunction is closely related to ovarian senility. It remains unclear whether MSCs can exert resistance to mitochondrial dysfunction induced by aging. Therefore, the ovarian mitochondrial membrane potential ($\Delta\Psi_m$) was measured using the JC-1 Assay Kit in the Oc + NS and Oc + BMSCs groups, and the fluorescence intensity was apparently enhanced in the Oc + BMSCs group compared with in the Oc + NS group after MSCs transplantation for four and eight weeks (Fig. 4B). Furthermore, we measured the expression levels of mitochondrial dynamics-related proteins (such as MFN1/2, OPA1, and DRP1) by western blotting and found that in the Oc + BMSCs group, the MFN1/2 and OPA1 expression levels were differentially increased and the DRP1 protein levels were significantly decreased compared to the Oc + NS group (Fig. 4C). Moreover, we quantified the mtDNA copy levels after MSCs transplantation in the Oc + NS and Oc + BMSCs groups and found that the amount of mtDNA levels increased approximately >2-fold from the ovaries in the Oc + NS group (Fig. 4D).

In addition, the transmission electron microscopy (TEM) examination of the mitochondrial ultrastructure of the ovaries in the two groups showed a conspicuous difference in the mitochondrial morphologies and number. In the Oc + NS group, the mitochondria presented a short rod-like structure and spheroids with fewer numbers, serious vacuolation and a disordered mitochondrial cristae arrangement (Fig. 4E, upper). Nevertheless, after MSCs transplantation in the Oc + BMSCs group, we could observe ameliorative mitochondrial cristae alignment and vacuolation, as well as a small number of long rod-like structures (Fig. 4E, lower).

MSCs reduced ovarian apoptosis induced by natural aging

TUNEL assay, western blotting and TEM were used to determine the cell apoptosis and the expression of apoptosis-related factors (such as Bcl-2, Bax, Caspase3 and Caspase9). Four and eight weeks after MSCs transplantation in mice, the average IntDen of TUNEL-positive ovarian cells in the Oc + BMSCs group were significantly weaker than that in the Oc + NS group (Fig. 5A/B, $P < 0.000$). In addition, the results of the ultrastructure from granulosa cells around oocytes in the Oc + NS group showed many apoptotic cells with nuclear shrinkage and severe cavitation; however, the apoptotic cells were clearly decreased in the Oc + BMSCs group as indicated by TEM observation (Fig. 5C). We further detected the expression of apoptosis-related proteins, and the western blotting indicated that the Bcl-2 expression levels were increased in the Oc + BMSCs group compared to the Oc + NS group, while the expression levels of Bax, Caspase3 and Caspase9 were decreased in the Oc + BMSCs group (Fig. 5D/E). The study indicated that the transplanted BMSCs^{MT/MT} could alleviate apoptosis induced by aging.

In situ repair abilities of human UC-MSCs on ovarian hypofunction caused by natural aging in rhesus monkeys with advanced age

After the highly purified UC-MSCs (5×10^6 UC-MSCs in 100 μ l normal saline for unilateral ovarian injection, the same amount for contralateral ovary, in accord with previously described [19]) were injected into ovaries for two months, the probe “Vysis SRY Probe LSI SRY Spectrum Orange/Vysis CEP X Spectrum Green” was used to mark the human umbilical cord-derived mesenchymal stem cells by a FISH technique. The results showed that male testicular tissue (Containing XY chromosome) was obtained as a positive control group with green/orange double signal, and control group derived-ovary was randomly selected as a negative control without positive signal. And the presence of a positive signal (green signal) in the ovaries was showed after HuMSCs treatment for 2 months

by FISH detection, suggesting that transplanted HuMSCs can locate into the ovarian tissues at least for 2 months (Fig. 6A). At two months after transplantation, E_2 level in Control Group decreased by 20.36% compared with that before transplantation (Pre-treatment), however, E_2 level only decreased by 3.72% in HuMSCs-treated Group compared with that before transplantation (Fig. 6B) without significant difference compared to that in Control Group. Meanwhile, the results showed that FSH levels increased significantly in Control Group at three months after transplantation compared with that before transplantation ($P < 0.01$), with rising much higher than 5 times (Fig. 6B). In HuMSCs-treated Group, FSH level increased by 78% compared with that before transplantation after transplantation for two months, and was significantly lower than that in Control Group ($P < 0.01$, Fig. 6B). With the advanced age, the total follicles in ovarian tissue of old rhesus monkeys were decreased significantly compared with that in young group (Young-Control) ($P < 0.05$, $P < 0.01$, Fig. 6C). Two months after HuMSCs transplantation, the total number of follicles was significantly higher than that in Control Group ($P < 0.05$, Fig. 6C). At four months after transplantation, the total number of follicles in the ovarian cortex was significantly lower than that in the younger group ($P < 0.01$), but still higher than that in Control Group (Fig. 6C). In addition, the number of follicles at all levels (primordial follicles, primary follicles and antral follicles) in old rhesus monkeys was significantly lower than that in young group ($P < 0.05$, Fig. 6D). Two months after HuMSCs transplantation, the number of follicles at all levels was significantly higher than that in Control Group ($P < 0.05$), especially the number of antral follicles was still significantly higher than that of the control group at four months after HuMSCs transplantation ($P < 0.05$, Fig. 6D). In addition, the ovarian ultrastructure in the control group and HuMSCs-treated group was also detected by transmission electron microscopy (TEM). The mitochondrial morphologies showed a conspicuous improvement with obvious mitochondrial cristae alignment and a small number of long rod-like structures displayed in the HuMSCs-treated group, compared with the short rod-like structure and spheroids, serious vacuolation and disordered mitochondrial cristae arrangement in the control group (Fig. 6E).

Discussion

It is established that ovarian functions decline with age in women, and there is a rapid loss of follicles before the reproductive stage and accelerated aging after 35 years old with no chance of pregnancy during menopause. Compared with other systems of the body, the ovary shows a prominent aging rate and different aging characteristics [5,6,30]. However, less information has been reported about ovarian reserve in the mouse. A study published in 2015 showed that the number of resting follicles displayed a rapid decline postnatal starting at day 21 until at least 20 weeks of age [31]. Thus, we chose 16, 20, 24, 28, 32, 36, and 40 weeks old C57BL/6J female mice for our experiments. Through observation, the pregnancy rate significantly decreased, accompanied by a prominent decrease in the average litter size of mice at 28w (28 weeks old). In addition, the FSH, LH, AMH, and E_2 levels markedly changed at 28w or 32w. As shown in our results, 32 weeks of age may be the optimal stage for MSCs therapy.

Considering the safety and patient financial burden, single transplantation was carefully recommended for the meaningful work. In our study, a preliminary assessment of MSCs' effect was performed about the three ways of transplantation commonly used, such as tail-intravenous, ovarian local injection and intraperitoneal injection. Significant effects and more sensitive changes were showed in the first two groups (tail-intravenous and ovarian local injection). Following highly purified MSCs trans-

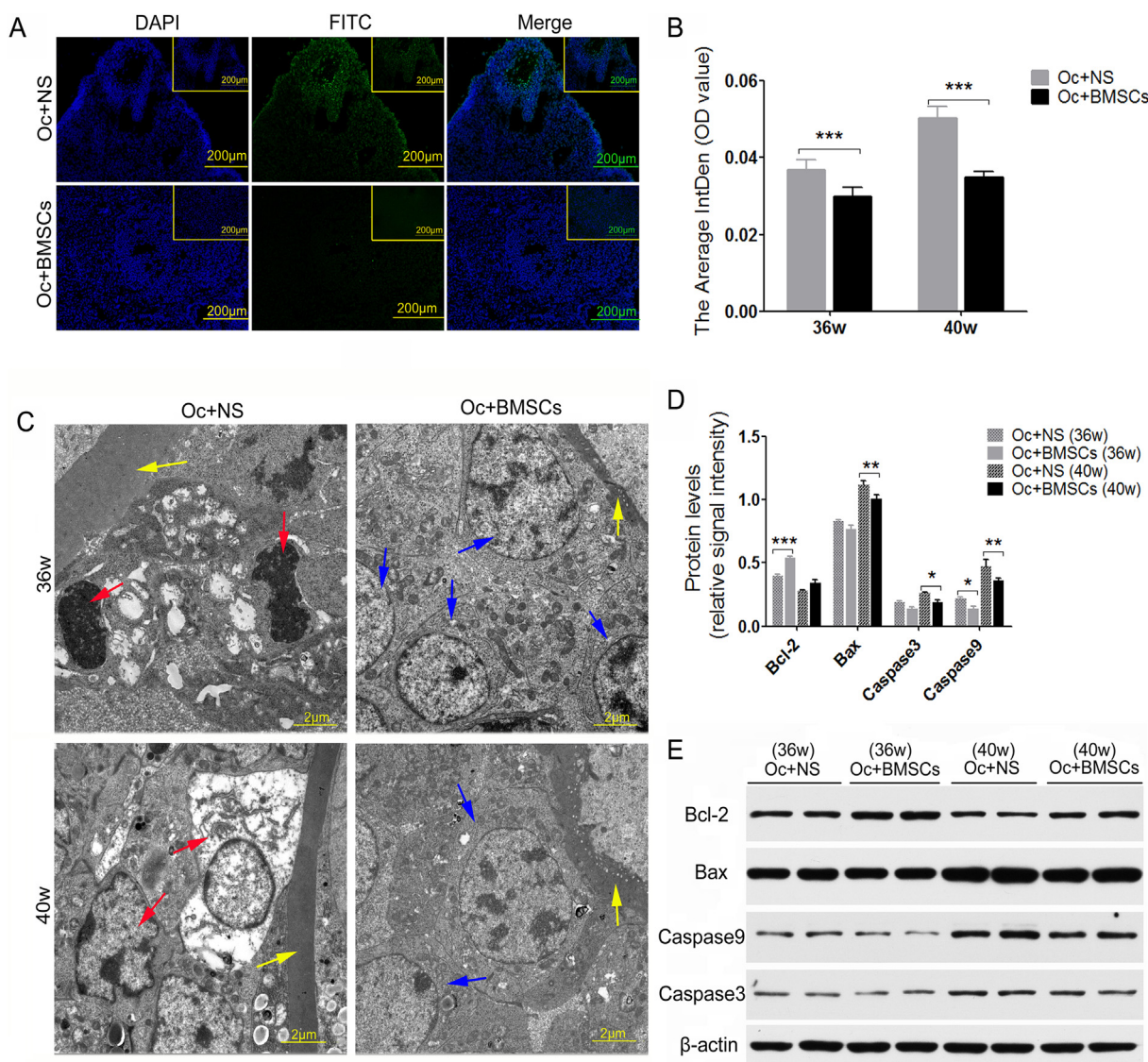


Fig. 5. The effect of transplanted MSCs on cell apoptosis of ovaries. (A and B) Representative images of TUNEL assay from ovarian tissue obtained from two groups of mice and the average IntDen of fluorescence intensity. Scale bar = 200 μ m. C Transmission electron microscopy results showing the granulosa cell apoptosis around oocytes. Scale bar = 2 μ m; zona pellucida (yellow arrow), granulosa cells (blue arrow), and apoptotic cells (red arrow). D Comparison between Bcl-2 and Bax, Caspase3 and Caspase9 protein levels. E The most representative images of western blotting for Bcl-2, Bax, Caspase3 and Caspase9 in two groups at 36w and 40w after BMSCs^{miT/mG} transplantation. * $P < 0.05$, ** $P < 0.01$, *** $P < 0.00$ vs. the Oc + NS group.

plantation by tail-intravenous and ovarian local injection at 32w, the immunofluorescence analysis indicated the successful MSCs homing to ovaries or the injection site for eight weeks post-transplantation (that is, 40 weeks of age) both in the Ti + BMSCs and Oc + BMSCs groups, which was in line with previous studies [32,33]. The ultimate fate of these cells will be the focus of the next step.

We observed changes in the hormone levels after MSCs transplantation by the two approaches. The current evidence suggests that MSCs made an earlier impact on the changes in hormone release after intravenous transplantation for four weeks, which may be related to the rapid action on the hypothalamic-pituitary-gonadal axis (HPG axis) and the limited number of stem cells homing to the ovaries later, in accordance with the slightly enlarged ovarian size after transplantation for six weeks. In contrast, MSCs exerted a remarkable effect on steroid hormones in the serum after transplantation for six weeks in the Oc + BMSCs group, which may be concerned with the sufficient number of stem cells located in the ovaries and subsequent feedback adjustment

with the HPG axis, which is in line with the earlier onset of a clear enlargement in the size of the ovaries after transplantation for four weeks and increased weight index of the ovaries, and exerted a conspicuous effect on improving ovarian function compared with transplantation via tail-intravenous injection.

The hormonal changes via the feedback of the hypothalamic-pituitary axis have a direct influence on the estrous cycle [34]. Our findings also demonstrated that transplanted MSCs could exhibit a more regular estrous cycle and exert a conspicuous effect in the Oc + BMSCs group according to the results of the number of estrous cycles, the percent of mice with an estrous cycle and the average duration of estrus, which are in accordance with the previously described hormonal changes. Furthermore, the pregnancy rate and the average litter size per pregnancy related to ovarian reserve further validated the conspicuous effect in the Oc + BMSCs group. In this study, irrespective of the invasion and surgical injury, the results indicated that the transplantation via ovarian local injection is more suitable for exerting resistance to ovarian hypofunction caused by natural aging and has a more

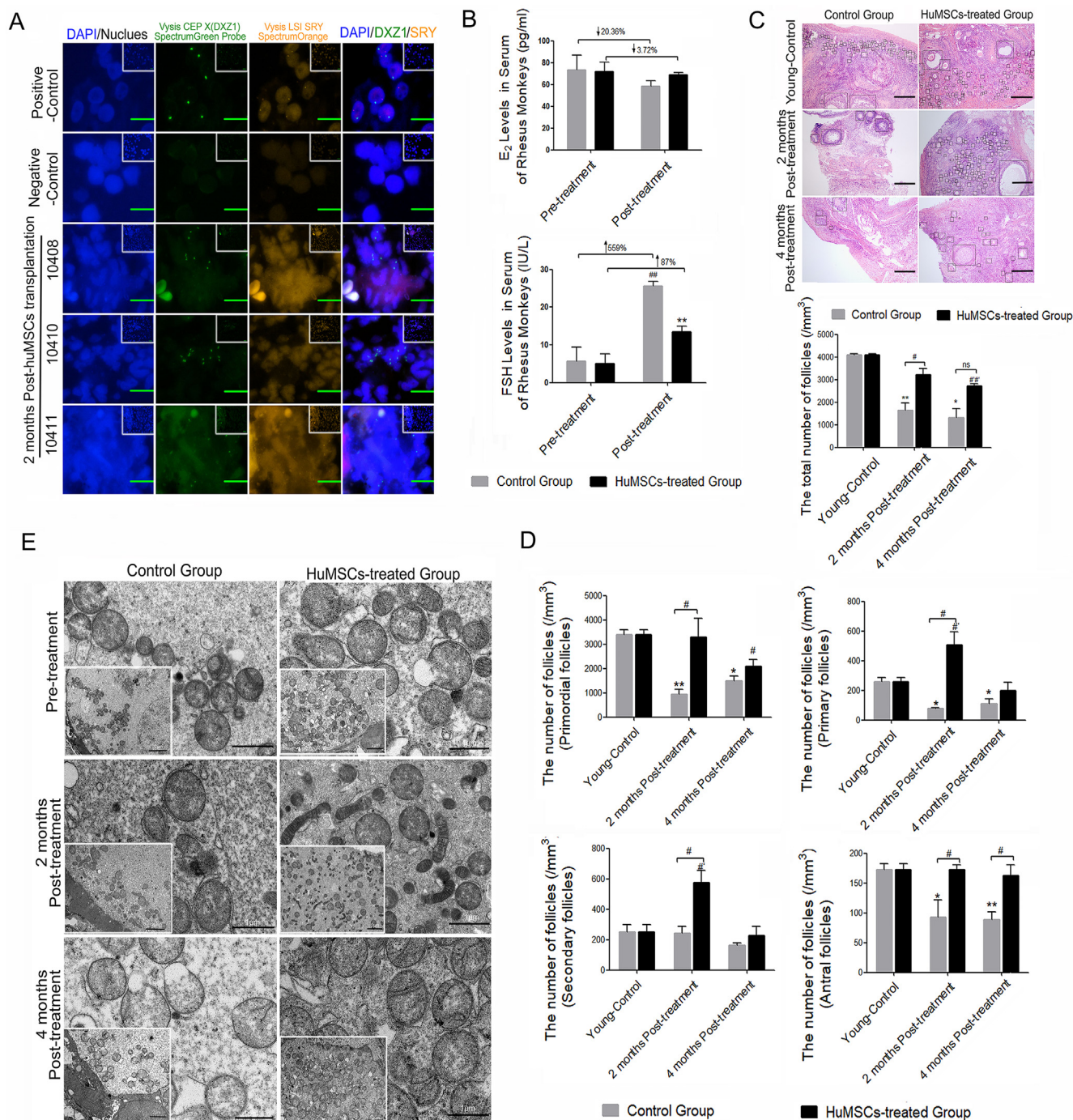


Fig. 6. In situ repair abilities of human UC-MSCs on ovarian hypofunction caused by natural aging in rhesus monkeys with advanced age. **A** FISH analysis for tracking transplanted HuMSCs in the ovaries. **B** The hormone levels of FSH and E₂ were measured by CLIA test at pre- or post-treatment in the control group and HuMSCs-treated group; † shows rising tendency and ‡ shows dropping amplitude compared with pre-treatment, ##*P* < 0.01 vs. pre-treatment, ***P* < 0.01 vs. the control group. **C** Representative images of ovarian morphology with HE-staining (Scale bar = 200 μm) and the comparison for total number of follicles. **P* < 0.05, ***P* < 0.01, ##*P* < 0.01 vs. Young-Control; #*P* < 0.05 vs. Control Group; ns: no statistical differences (vs. Control Group). **D** The comparison for the number of follicles at all levels. **P* < 0.05, ***P* < 0.01, #*P* < 0.05 vs. Young-Control; #*P* < 0.05 vs. Control Group. **E** Representative image of mitochondrial ultrastructure detected by TEM (Scale bar = 1 μm); White square represents low power of mitochondria (Scale bar = 2 μm).

prominent effect for at least one month after a single injection; however, these data are in contrast to a previous report published in 2016 [35].

Nevertheless, the current evidence may suggest the different mechanisms that occur on ovaries by tail-intravenous and ovarian local injection, and the time of localization and quantity of stem cells may play a decisive role in delaying ovarian senility and saving infertility induced by age; however, the detailed mechanism

remains unclear. In our study, all measured outcomes indicated that MSCs transplantation into mice could improve fertility potential relevant to ovarian reserve. Moreover, as previously indicated, the diminished ovarian reserve with increasing age will be in connection with the decreased quantity and aberrant quality of oocytes [5,6]. In line with our expected result, transplanted MSCs could increased growing follicles in the early stages of transplantation, which may be associated with limited storage of

the follicular pool, and promote maturation with a high level of antral follicle count after MSCs transplantation for eight weeks, which may be related to the decreased follicular atresia. Moreover, after the MSCs treatment, not only the quantity of follicles were increased, the oocyte quality also recovered as expected, including the increased rate of fertilization, cleavage and embryo formation and the decreased aberrant changes in the spindle apparatus and chromosome alignment, as well as the descending percentage of aneuploidy and increased polarity distribution of mitochondria to provide necessary energies for the fertilization and following process. However, there was no significant difference in the age-related poor developmental potential and arrested meiosis of oocytes during the post-transplanted stages of MSCs, and we speculate these findings may be related to the gradually decreased localization and quantity of stem cells, an insufficient number of samples or irreparable oocyte aging.

Anti-apoptosis was likely to be the next relevant mechanism in the process of the *in vivo* effect of MSCs treatment, which has been preliminarily validated by our previous finding regarding the decreased follicular atresia. Further study showed that the number of TUNEL-positive cells significantly decreased, the Bcl-2 expression levels were increased and the expression levels of Bax, Caspase3 and Caspase9 were decreased, even with ameliorative nuclear shrinkage and severe cavitation in granulosa cells around oocytes. Moreover, the mitochondrial function is considered to be another underlying factor that affects oocyte quality [20,21], and the further evidence regarding a series of mitochondrial function detection suggests that MSCs treatment could exert resistance to mitochondrial dysfunction induced by aging with an enhanced mitochondrial membrane potential, increased mtDNA copies, improved expression of mitochondrial dynamics-related proteins, and ameliorative mitochondrial cristae alignment and vacuolation, as well as the appearance of a small number of long rod-like structures.

Over the investigation, MSCs transplantation by ovarian local injection has been confirmed to exert more remarkable resistance to ovarian hypofunction caused by natural aging via ameliorating the follicle development and quality, and mechanisms of improving mitochondrial function and anti-apoptosis also have been explored. Importantly, the long-term effect of stem cells *in vivo* (such as differentiation and tumorigenic potential) has been initially assessed to be safe for at least six months after transplantation. In addition, the same repair abilities have been also confirmed in nonhuman primates, and the results were verified consistent with the previous results of rodent experiments. Our data could provide guidance for the clinical transformation of stem cells, at least with respect to female fertility protection and rescuing ovarian aging. In the next step, further and deeper studies should be needed, that aim to better understand the exact mechanism of the therapeutic potential of stem cells.

Conclusion

MSCs transplantation into ovaries for at least one month by ovarian local injection could exert most conspicuous effect on antagonizing age-associated ovarian hypofunction without significant found of tumorigenicity which suggested the potential value of stem cells in ovarian natural aging providing a new strategy for female fertility preservation and a great guidance for future clinical and translational research

Compliance with Ethics requirements

All procedures followed were in accordance with the National Research Council's "Guideline for the Care and Use of Laboratory Animals".

CRedit authorship contribution statement

Lingjuan Wang: Conceptualization, Methodology, Investigation, Project administration, Writing - original draft. **Qiaojuan Mei:** Validation, Formal analysis, Visualization. **Qin Xie:** Software. **Huiying Li:** Formal analysis. **Ping Su:** Resources, Data Curation. **Ling Zhang:** Resources, Data Curation. **Kezhen Li:** Resources. **Ding Ma:** Writing - review & editing. **Gang Chen:** Resources, Writing - review & editing. **Jing Li:** Writing - review & editing. **Wenpei Xiang:** Conceptualization, Data Curation, Supervision, Project administration, Funding acquisition.

Declaration of Competing Interest

The authors declare that they have no known competing financial interests or personal relationships that could have appeared to influence the work reported in this paper.

Acknowledgments

We acknowledge the Institute of Fujian Experiment Center of Non-human Primate for Family Planning for breeding and supplying the rhesus monkey animal model; We thank Chuanhu Yu and Chengliang Xiong from the Center of Reproductive Medicine, Tongji Medical College, Huazhong University of Science and Technology for the operation of open abdominal surgery and providing guidance for important intellectual content.

Funding

This work was supported by the National Key Research and Development Program of China (2017YFC1002002) and the Project funded by China Postdoctoral Science Foundation (2020M682423). The funders played no role in the study design, data collection and analysis, decision to publish, or preparation of the manuscript.

Appendix A. Supplementary material

Supplementary data to this article can be found online at <https://doi.org/10.1016/j.jare.2021.09.001>.

References

- [1] Eijkemans MJC, van Poppel F, Habbema DF, Smith KR, Leridon H, te Velde ER. Too old to have children? Lessons from natural fertility populations. *Human Reproduction* 2014;29(6):1304–12. doi: <https://doi.org/10.1093/humrep/deu056>.
- [2] American College of Obstetricians and Gynecologists Committee on Gynecologic Practice and Practice Committee. Female age-related fertility decline. Committee Opinion No. 589. *Fertil Steril*. 2014 Mar;101(3):633–4. doi: 10.1016/j.fertnstert.2013.12.032.
- [3] Zegers-Hochschild F, Adamson GD, Dyer S, Racowsky C, de Mouzon J, Sokol R, et al. The International Glossary on Infertility and Fertility Care, 2017. *Fertil Steril* 2017;108(3):393–406. doi: <https://doi.org/10.1016/j.fertnstert.2017.06.005>.
- [4] Broekmans FJ, Soules MR, Fauser BC. Ovarian aging: mechanisms and clinical consequences. *Endocr Rev* 2009;30(5):465–93. doi: <https://doi.org/10.1210/er.2009-0006>.
- [5] Farquhar CM, Bhattacharya S, Repping S, Mastenbroek S, Kamath MS, Marjoribanks J, et al. Female subfertility. *Nat Rev Dis Primers*. 2019;5(1). doi: <https://doi.org/10.1038/s41572-018-0058-8>.
- [6] Li Q, Geng XD, Zheng W, Tang J, Xu B, Shi QH. Current understanding of ovarian aging. *Science China-Life Sci* 2012;55(8):659–69. doi: <https://doi.org/10.1007/s11427-012-4352-5>.
- [7] te Velde ER, Pearson PL. The variability of female reproductive ageing. *Hum Reprod Update* 2002;8(2):141–54. doi: <https://doi.org/10.1093/humupd/8.2.141>.
- [8] Baird DT, Collins J, Egozcue J, Evers LH, Gianaroli L, Leridon H, et al. Fertility and ageing. *Human Reprod Update* 2005;11(3):261–76. doi: <https://doi.org/10.1093/humupd/dmi006>.
- [9] Mascarenhas MN, Flaxman SR, Boerma T, Vanderpoel S, Stevens GA. National, regional, and global trends in infertility prevalence since 1990: a systematic

- analysis of 277 health surveys. *PLoS Med.* 2012;9(12). doi: <https://doi.org/10.1371/journal.pmed.1001356>.
- [10] Nelson SM, Telfer EE, Anderson RA. The ageing ovary and uterus: new biological insights. *Human Reproduct Update* 2013;19(1):67–83. doi: <https://doi.org/10.1093/humupd/dms043>.
- [11] Malchau SS, Henningsen AA, Loft A, Rasmussen S, Forman J, Nyboe Andersen A, et al. The long-term prognosis for live birth in couples initiating fertility treatments. *Human Reproduct (Oxford, England)*. 2017;32(7):1439–49. doi: <https://doi.org/10.1093/humrep/dex096>.
- [12] Hikabe O, Hamazaki N, Nagamatsu Go, Obata Y, Hirao Y, Hamada N, et al. Reconstitution in vitro of the entire cycle of the mouse female germ line. *Nature* 2016;539(7628):299–303. doi: <https://doi.org/10.1038/nature20104>.
- [13] Li J, Kawamura K, Cheng Y, Liu S, Klein C, Liu S, et al. Activation of dormant ovarian follicles to generate mature eggs. *Proc Natl Acad Sci U S A* 2010;107(22):10280–4. doi: <https://doi.org/10.1073/pnas.1001198107>.
- [14] Zhai J, Yao G, Dong F, Bu Z, Cheng Y, Sato Y, et al. In Vitro Activation of Follicles and Fresh Tissue Auto-transplantation in Primary Ovarian Insufficiency Patients. *J Clin Endocrinol Metabol* 2016;101(11):4405–12. doi: <https://doi.org/10.1210/ic.2016-1589>.
- [15] Lee H-J, Selesniemi K, Niikura Y, Niikura T, Klein R, Dombkowski DM, et al. Bone marrow transplantation generates immature oocytes and rescues long-term fertility in a preclinical mouse model of chemotherapy-induced premature ovarian failure. *J Clin Oncol* 2007;25(22):3198–204. doi: <https://doi.org/10.1200/JCO.2006.10.3028>.
- [16] Takehara Y, Yabuuchi A, Ezoe K, Kuroda T, Yamadera R, Sano C, et al. The restorative effects of adipose-derived mesenchymal stem cells on damaged ovarian function. *Lab Invest* 2013;93(2):181–93. doi: <https://doi.org/10.1038/labinvest.2012.167>.
- [17] Ghadami M, El-Demerdash E, Zhang D, Salama SA, Binhazim AA, Archibong AE, et al. Bone marrow transplantation restores follicular maturation and steroid hormones production in a mouse model for primary ovarian failure. *PLoS One* 2012;7(3). doi: <https://doi.org/10.1371/journal.pone.0032462>.
- [18] Terraciano P, Garcez T, Ayres L, Durlí I, Baggio M, Kuhl CP, et al. Cell therapy for chemically induced ovarian failure in mice. *Stem Cells Int* 2014;2014:1–8. doi: <https://doi.org/10.1155/2014/720753>.
- [19] Ding L, Yan G, Wang B, Xu Lu, Gu Y, Ru T, et al. Transplantation of UC-MSCs on collagen scaffold activates follicles in dormant ovaries of POF patients with long history of infertility. *Sci China Life Sci* 2018;61(12):1554–65. doi: <https://doi.org/10.1007/s11427-017-9272-2>.
- [20] Wai T, Ao A, Zhang X, Cyr D, Dufort D, Shoubridge EA. The role of mitochondrial DNA copy number in mammalian fertility. *Biol Reprod* 2010;83(1):52–62. doi: <https://doi.org/10.1095/biolreprod.109.080887>.
- [21] He Y-H, Lu X, Wu H, Cai W-W, Yang L-Q, Xu L-Y, et al. Mitochondrial DNA content contributes to healthy aging in Chinese: a study from nonagenarians and centenarians. *Neurobiol Aging* 2014;35(7):1779.e1–e4. doi: <https://doi.org/10.1016/j.neurobiolaging.2014.01.015>.
- [22] Ben-Meir A, Yahalomi S, Moshe B, Shufaro Y, Reubinoff B, Saada A. Coenzyme Q-dependent mitochondrial respiratory chain activity in granulosa cells is reduced with aging. *Fertil Steril* 2015;104(3):724–7. doi: <https://doi.org/10.1016/j.fertnstert.2015.05.023>.
- [23] Tatone C, Amicarelli F. The aging ovary—the poor granulosa cells. *Fertil Steril* 2013;99(1):12–7. doi: <https://doi.org/10.1016/j.fertnstert.2012.11.029>.
- [24] Iwata H. Age-associated changes in granulosa cells and follicular fluid in cows. *J Reproduct Develop* 2017;63(4):339–45. doi: <https://doi.org/10.1262/jrd.2017-048>.
- [25] Wu YG, Barad DH, Kushnir VA, Lazzaroni E, Wang Q, Albertini DF, et al. Aging-related premature luteinization of granulosa cells is avoided by early oocyte retrieval. *J Endocrinol* 2015;226(3):167–80. doi: <https://doi.org/10.1530/JOE-15-0246>.
- [26] Liu Y, Han M, Li X, Wang H, Ma M, Zhang S, et al. Age-related changes in the mitochondria of human mural granulosa cells. *Human Reproduct (Oxford, England)*. 2017;32(12):2465–73. doi: <https://doi.org/10.1093/humrep/dex309>.
- [27] Wang L, Song S, Liu X, Zhang M, Xiang W. Low MFN2 expression related to ageing in granulosa cells is associated with assisted reproductive technology outcome. *Reprod Biomed Online* 2019;38(2):152–8. doi: <https://doi.org/10.1016/j.rbmo.2018.10.011>.
- [28] Su J, Ding L, Cheng J, Yang J, Li X, Yan G, et al. Transplantation of adipose-derived stem cells combined with collagen scaffolds restores ovarian function in a rat model of premature ovarian insufficiency. *Hum Reprod* 2016;31(5):1075–86. doi: <https://doi.org/10.1093/humrep/dew041>.
- [29] Zhao Y, Ma J, Yi P, Wu J, Zhao F, Tu W, et al. Human umbilical cord mesenchymal stem cells restore the ovarian metabolome and rescue premature ovarian insufficiency in mice. *Stem Cell Res Ther* 2020;11(1). doi: <https://doi.org/10.1186/s13287-020-01972-5>.
- [30] Perheentupa A, Huhtaniemi I. Aging of the human ovary and testis. *Mol Cell Endocrinol* 2009;299(1):2–13. doi: <https://doi.org/10.1016/j.mce.2008.11.004>.
- [31] Gaytan F, Morales C, Leon S, Garcia-Galiano D, Roa J, Tena-Sempere M. Crowding and follicular fate: spatial determinants of follicular reserve and activation of follicular growth in the mammalian ovary. *PLoS One* 2015;10(12). doi: <https://doi.org/10.1371/journal.pone.0144099>.
- [32] Chen X, Lu M, Ma N, Yin G, Cui C, Zhao S. Dynamic tracking of injected mesenchymal stem cells after myocardial infarction in rats: A Serial 7T MRI study. *Stem Cells Int* 2016;2016:1–10. doi: <https://doi.org/10.1155/2016/4656539>.
- [33] Song D, Zhong Y, Qian C, Zou Q, Ou J, Shi Y, et al. Human umbilical cord mesenchymal stem cells therapy in cyclophosphamide-induced premature ovarian failure rat model. *Biomed Res Int* 2016;2016:1–13. doi: <https://doi.org/10.1155/2016/2517514>.
- [34] Chakraborty TR, Donthireddy L, Adhikary D, Chakraborty S. Long-term high fat diet has a profound effect on body weight, hormone levels, and Estrous cycle in mice. *Med Sci Monit* 2016;22:1601–8. doi: <https://doi.org/10.12659/msm.897628>.
- [35] Zhang J, Xiong J, Fang L, Lu Z, Wu M, Shi L, et al. The protective effects of human umbilical cord mesenchymal stem cells on damaged ovarian function: A comparative study. *Bioscience Trends* 2016;10(4):265–76. doi: <https://doi.org/10.5582/bst.2016.01125>.